AD-A040 312 LARGE CALIBER WEAPON SYSTEMS LAB (ARMY) DOVER N J F/G 19/1
POST-ENGRAVING STRESS ANALYSIS OF A PLASTIC ROTATING BAND.(U)
APR 77 Y CHEN
UNCLASSIFIED ARLCD-TR-77004 NL

| OF |

AD A040312

END
DATE
FILMED
7-77

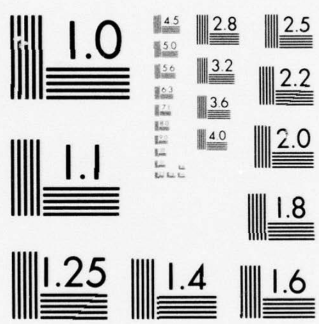
1.0
1.1
1.25
1.4
1.6
1.8
2.0
2.2
2.5
2.8
3.2
3.6
4.0
4.5
5.0
5.6
6.3

12

AD

COPY NO. 16

TECHNICAL REPORT ARLCD-TR-77004

POST-ENGRAVING STRESS ANALYSIS OF A PLASTIC ROTATING BAND

YU CHEN

APRIL 1977

U.S. ARMY ARRADCOM
US ARMY ARMAMENT RESEARCH AND DEVELOPMENT COMMAND
LARGE CALIBER
WEAPON SYSTEMS LABORATORY
DOVER, NEW JERSEY

The findings in this report are not to be construed as an official Department of the Army position.

DISPOSITION

Destroy this report when no longer needed. Do not return to the originator.

UNCLASSIFIED

SECURITY CLASSIFICATION OF THIS PAGE (When Data Entered)

REPORT DOCUMENTATION PAGE

READ INSTRUCTIONS BEFORE COMPLETING FORM

1. REPORT NUMBER 9 14

Technical Report ARLCD-TR-77004

2. GOVT ACCESSION NO.

3. RECIPIENT'S CATALOG NUMBER

4. TITLE (and Subtitle) 6

POST-ENGRAVING STRESS ANALYSIS OF A PLASTIC ROTATING BAND.

5. TYPE OF REPORT & PERIOD COVERED

6. PERFORMING ORG. REPORT NUMBER

7. AUTHOR(s) 10

Yu Chen

8. CONTRACT OR GRANT NUMBER(s)

AMCMS 6121.05.11H8.4

9. PERFORMING ORGANIZATION NAME AND ADDRESS

Materials Engineering Division, FRL
Picatinny Arsenal
Dover, NJ 07801

10. PROGRAM ELEMENT, PROJECT, TASK AREA & WORK UNIT NUMBERS

12 37p.

11. CONTROLLING OFFICE NAME AND ADDRESS

ARRADCOM, Large Caliber Weapon Systems Lab
Applied Sciences Div, Organic Materials Br
Dover, NJ 07801

12. REPORT DATE 11

Apri[redacted]977

13. NUMBER OF PAGES

38

14. MONITORING AGENCY NAME & ADDRESS (if different from Controlling Office)

15. SECURITY CLASS. (of this report)

Unclassified

15a. DECLASSIFICATION/DOWNGRADING SCHEDULE

16. DISTRIBUTION STATEMENT (of this Report)

Approved for public release, distribution unlimited.

17. DISTRIBUTION STATEMENT (of the abstract entered in Block 20, if different from Report)

18. SUPPLEMENTARY NOTES

19. KEY WORDS (Continue on reverse side if necessary and identify by block number)

Rotating band analysis
Non-metallic rotating bands
Rotating band stresses
Ballistic cycle
Internal ballistics

20. ABSTRACT (Continue on reverse side if necessary and identify by block number)

Certain simplifying assumptions are made in order to calculate the stress history induced in a plastic rotating band as a result of its internal ballistic flight.

DD FORM 1 JAN 73 1473 EDITION OF 1 NOV 65 IS OBSOLETE

UNCLASSIFIED

SECURITY CLASSIFICATION OF THIS PAGE (When Data Entered)

410 163 mt

TABLE OF CONTENTS

OBJECT

The object of the effort covered in this report is to analyze the stresses induced in the plastic rotating band during the time in which the projectile travels inside the gun after it has been engraved. In this period the acceleration of the projectile causes radial and circumferential, as well as axial normal stresses. Shearing stresses are also generated in two directions. The assessment of the levels of stresses in the rotating band not only will furnish necessary information in the selection of the plastic materials, it also will shed light on the gun wear problem because the contact pressure between the surfaces of the gun and the rotating band is also determined by the analyses.

An axisymmetric model of the rotating band in flight inside the gun after it has passed the forcing cone has been formulated and analyzed mathematically. The analytical solutions of stress components were then used in a sample calculation based on a sample material with E = 6895 MPa (1,000,000 psi) and a sample geometry of a 105 mm gun. Results show that the maximum compressive stress at the interface of the gun and the rotating band is about 110 MPa (16,000 psi) whereas at the band seat a tensile stress of about the same magnitude is induced. Shearing stresses are only of the order of 0.7 MPa (several hundred psi). It is observed that due to the assumption of the rigidity of the gun and the shell body the normal stresses are higher than the actual stresses. The stress-free conditions assumed for the circumferential and axial displacements cause the shearing stress to be too low. Refinements of the mathematical model currently in use will not be a major undertaking and are recommended.

INTRODUCTION

In the design of a plastic rotating band, the design analysis can be arbitrarily divided into three separate stages. The first stage is to deal with the engraving process. As the rotating band enters the forcing cone the outside diameter of the band is compressed at first and then engraved by the lands on the gun tube. The objective of the analysis of this stage of action is to determine the pressure exerted on the gun tube by the rotating band as it is being engraved. The second stage of analysis deals with the dynamics and the stress problems occurring after the projectile has emerged from the forcing cone and during its travel through the gun tube. It ends at the instant the projectile leaves the muzzle of the gun. The third stage refers to the problems relating to the band during the free flight of the projectile (Fig 1).

After the rotating band has been engraved by the forcing cone the projectile is made to accelerate through the gun both axially and circumferentially, acquiring the desired muzzle velocity and spin at its completion of the travel inside the gun. During this period, pressure is generated between the mating surfaces of the band and the barrel due to the inertial forces acting on the band. This pressure has direct influence on the frictional force which exists at the interface of the radial contact. It therefore determines the wear of the mating surfaces. Besides the radial contacts there are the lateral contacts between the band and the gun barrel. Very high contact pressure exists there due to the angular acceleration of the projectile. These pressures and the stresses induced in the band during the post engraving period are the subject of analysis of this paper.

The actual problem of stress analysis of the rotating band during its travel in the gun is a complicated one. Foremost among the complexities involved is the geometry of the mating surfaces of the band in contact with the gun. These surfaces are in the form of lands and grooves after the band has been engraved. Since the gun barrel and the shell body both deform, though to a much lesser extent compared to the deformation of the band, to analyze the stresses in the band one needs also to analyze the deformations of the gun and the shell. The complete formulation thus involves three problems (the gun, the band, and the shell) coupled together. Simplifications must be made before analysis can proceed.

In the following analysis the rotating band is considered to be a smooth cylindrical shell instead of the serrated configuration. This assumption ignores the lateral surfaces of the land and thus the stress variations due to the irregularities in the circumferential

direction. Such calculation should give a meaningful estimate of the order of magnitude of the stress levels at the contact. This estimation of stress level would be useful in the selection of materials suitable for the application with regard to their strengths and wear resistances. A second assumption is to ignore the deformations of the gun and the shell so as to decouple the problem of the band deformation. This means that in the analysis we either take the deformations of the gun and the shell to the zero or use some predetermined values for these deformations, say from some experiments.

Besides the assumptions made above, it will be assumed that the rotating band under the given load is stressed within the elastic limit. Therefore the subsequent analysis will be based on the theory of elasticity.

MATHEMATICAL ANALYSIS

According to the theory of elasticity three equations of motion in the cylindrical coordinates r, θ, and z are as follows (Ref 1):

$$(\lambda+2\mu)\frac{\partial\Theta}{\partial r} + \mu\frac{\partial}{\partial z}\left(\frac{\partial u}{\partial z} - \frac{\partial w}{\partial r}\right) = \rho\, a_r$$

$$\frac{\mu}{r}\frac{\partial^2 v}{\partial z^2} + \mu\frac{\partial}{\partial r}\left(\frac{\partial(rv)}{r\partial r}\right) = \rho\, a_\theta \qquad (1)$$

$$(\lambda+2\mu)\frac{\partial\Theta}{\partial z} - \mu\frac{\partial}{r\partial r}\left[r\left(\frac{\partial u}{\partial z} - \frac{\partial w}{\partial r}\right)\right] = \rho a_z$$

where $$\Theta = \frac{1}{r}\frac{\partial(ru)}{\partial r} + \frac{\partial v}{r\partial\Theta} + \frac{\partial w}{\partial z} \qquad (2)$$

and u, v, w are the displacements in the radial (r), circumferential (Θ), and axial (z) directions of a point on the band, referring to a frame of reference rotating with the band, and a_r, a_Θ, a_z are the acceleration components.

Let the angular velocity and the angular acceleration be ω and $\dot{\omega}$, the rifling angle be δ and the outer radius of the band be b. The components of the acceleration of a point on the band as observed from a laboratory frame of reference are calculated as:

$$a_r = -r\omega^2 - 2\omega \frac{\partial v}{\partial t} + \frac{\partial^2 u}{\partial t^2}$$

$$a_\Theta = r\dot{\omega} + \frac{\partial^2 v}{\partial t^2} + 2\omega \frac{\partial u}{\partial t} \tag{3}$$

$$a_z = \left(\frac{b}{tg\delta}\right)\dot{\omega} + \frac{\partial^2 w}{\partial t^2}$$

To further facilitate the analysis, the band is assumed to be in plane strain; thus the z coordinate can be ignored. It is further observed that the displacements are independent of their angular positions. This means that the θ coordinate can also be ignored. The remaining independent variables are the radial distance r and the time t.

Using all the above assumptions and substituting Equation (3) into Equation (1) we obtain the one-dimensional time-dependent model of the rotating band as described by the following three partial differential equations.

$$(\lambda+2\mu)\ \frac{\partial}{\partial r}\left[\frac{1}{r}\ \frac{\partial(ru)}{\partial r}\right] = \rho\frac{\partial^2 u}{\partial t^2} - 2\rho\omega\frac{\partial v}{\partial t} - \rho r\omega^2$$

$$\mu\frac{\partial}{\partial r}\left[\frac{1}{r}\ \frac{\partial(rv)}{\partial r}\right] = \rho\frac{\partial^2 v}{\partial t^2} + 2\rho\omega\frac{\partial u}{\partial t} + \rho r\dot{\omega} \tag{4}$$

$$\mu\left(\frac{\partial^2 w}{\partial r^2} + \frac{1}{r}\ \frac{\partial w}{\partial r}\right) = \rho\frac{\partial^2 w}{\partial t^2} + \rho\left(\frac{b}{tg\delta}\right)\dot{\omega}$$

It can be seen that the first and the second equations of Equation (4) are coupled through the Coriolis terms.

Corresponding to Equation (4) a system of boundary conditions must be prescribed to depict the physical conditions existing at the inner and the outer contact surfaces of the band. For the radial displacement the boundary conditions state that its values must vanish or be equal to some predetermined constants. These constants can be selected from some known data pertaining to the particular ordnance system in consideration, i.e., $u(a) = u(b) = 0$, or $u(a) = A$, $u(b) = B$, where a and b are the inner and the outer radii of the band, and A and B are the predetermined values of deformation of the inner and the outer surfaces.

For the circumferential displacement v the boundary conditions are $v(a) = 0$, which corresponds to the condition of no relative motion at the interface between the band and the shell, and $v(b)$ being unspecifiable. At the contact between the band and the gun either the interface can be assumed to be stress free or a predetermined frictional stress can be assumed. The boundary conditions for the axial components w are similar to those of v.

In Equation (4) the angular velocity and the angular acceleration are given functions of time. For each ammunition system, depending on the condition of the gun and the zone of firing, the interior ballistic performances vary. Some typical data will be used in the analysis to get representative answers which will disclose the stress levels induced in the particular system.

The individual equations in Equation (4) are similar in their structure. To determine the displacements due to the imposed inertial forces, one must solve for the particular solutions due to the inertial forces. To accomplish this the homogeneous solutions must be obtained first. This can be accomplished by the separation of variables technique.

The Radial Displacement, u(r,t)

Let

$$u(r,t) = U(r)\sin\alpha t \tag{5}$$

Substituting Equation (5) into the first equation of Equation (4), with the Coriolis term dropped, yields the following equation:

$$\frac{d^2U}{dr^2} + \frac{1}{r}\frac{dU}{dr} + (\beta^2 - \frac{1}{r^2})U = 0 \tag{6}$$

where $$\beta^2 = \frac{\rho}{\lambda + 2\mu}\alpha^2 .$$

The homogeneous part of Equation (6) is the Bessel's equation of the first order, whose solution can be written in the form

$$U(r) = A_1 J_1(\beta r) + A_2 Y_1(\beta r) \tag{7}$$

where J_1 and Y_1 are the Bessel's functions of the first and the second kind. The subscripts denote the order of the Bessel's function.

Upon imposing the boundary conditions

$$U(a) - U(b) = 0 \tag{8}$$

the eigenvalue equation is obtained.

$$J_1(\beta a)\, Y_1(\beta b) - J_1(\beta b)\, Y_1(\beta a) = 0 \tag{9}$$

If a new variable $\overline{\beta} = \beta a$ and a parameter $k = b/a$ are introduced, then Equation (9) can be cast in the form of

$$J\,(\overline{\beta})\; Y\,(k\overline{\beta}) - J\,(k\overline{\beta})\; Y\,(\overline{\beta}) = 0 \tag{10}$$

Since there is no available information regarding the eigenvalues of this equation, numerical solutions will be performed to obtain the eigenvalues. These values are needed for subsequent calculations.

Assuming the eigenvalues are $\overline{\beta}_n$, the set of orthogonal functions corresponding to the set of $\overline{\beta}_n$ are given by

$$\psi(\overline{\beta}_n \frac{r}{a}) = J_1(\overline{\beta}_n \frac{r}{a}) - K\, Y_1(\overline{\beta}_n \frac{r}{a}) \tag{11}$$

where $$K = \frac{J_1(\overline{\beta}_n)}{Y_1(\overline{\beta}_n)} = \frac{J_1(k\overline{\beta}_n)}{Y_1(k\overline{\beta}_n)}$$

a relation derivable from Equation (10).

To solve the inhomogeneous problem, Green's function method will be employed. Let $\phi(r,t)$ be a general representation of the inhomogeneous terms in Equation (4). The particular solution in terms of ϕ can be represented by the following integral.

$$\bar{u}(r,t) = \int_0^t \int_a^b G(r,\xi,t-\tau)\phi(\xi,\tau)d\xi d\tau \tag{12}$$

where $G(r,\xi,t-\tau)$ is Green's function of the partial differential equation.

Substituting Equation (12) in the first equation of Equation (4) yields

$$(\lambda+2\mu) \int\int \frac{\partial}{\partial r}[\frac{1}{r} \frac{\partial(rG)}{\partial r}]\phi(\xi,\tau)d\xi d\tau$$

$$- \rho \int\int \frac{\partial^2 G}{\partial t^2} \phi(\xi,\tau)d\xi d\tau = \phi(r,t)$$

from which it can be seen that

$$(\lambda+2\mu) \frac{\partial}{\partial r}[\frac{1}{r} \frac{\partial(rG)}{\partial r}] - \rho\frac{\partial^2 G}{\partial t^2} = \delta(r-\xi)\delta(t-\tau) \tag{13}$$

in which the right hand side is the product of two Dirac-delta functions.

To determine Green's function $G(r,\xi,t-\tau)$ it is necessary to expand the delta function in the spatial variable into an infinite series in the orthogonal function $\psi(\bar{\beta}_n \frac{r}{a})$.

Letting

$$\delta(r-\xi) = \sum_{n=1}^{\infty} A_n(\xi)\xi\psi(\bar{\beta}_n \frac{r}{a}) \tag{14}$$

and due to the orthogonality relation existing between ψ-functions corresponding to different $\bar{\beta}_n$, i.e.,

$$\int_a^b \xi\psi(\bar{\beta}_n\frac{\xi}{a})\psi(\bar{\beta}_n \frac{\xi}{a})d\xi = 0$$

we obtain

$$A_n = \frac{\psi(\overline{\beta}_n \frac{r}{a})}{N} \tag{15}$$

where

$$N = \int_0^b \xi\psi^2(\overline{\beta}_n \frac{\xi}{a})d\xi$$

To separate variables in Equation (13) we assume that

$$G(r,\xi,t-\tau) = \sum_{n=1}^{\infty} \frac{1}{N}B_n(t-\tau)\xi\psi(\overline{\beta}_n \frac{r}{a})\psi(\overline{\beta}_n \frac{\xi}{a}) \tag{16}$$

Substituting Equation (16) into Equation (13) and using the fact that $(\psi(\overline{\beta}_n \frac{r}{a})$ satisfies the homogeneous part of Equation (6) yields an ordinary differential equation in

$$\frac{d^2B_n}{d\ t^2} + \alpha_n{}^2B_n = -\frac{1}{\rho}\ \delta(t-\tau) \tag{17}$$

Equation (17) has the following solution

$$B_n(t-\tau) = -\frac{1}{\rho\alpha_n}\ \sin\alpha_n(t-\tau) \tag{18}$$

Finally,

$$G(r,\xi,t-\tau) = \sum_{n=1}^{\infty} -\frac{\xi\psi(\overline{\beta}_n \frac{r}{a})\psi(\overline{\beta}_n \frac{\xi}{a})}{\rho N\alpha_n} \sin\alpha_n(t-\tau) \tag{19}$$

and if $\phi(r,t) = -\rho r\omega^2$

$$\overline{u}(r,t) = \int_0^t \int_a^b \sum_{n=1}^{\infty} \frac{\xi\psi(\overline{\beta}_n \frac{r}{a})\psi(\overline{\beta}_n \frac{\xi}{a})}{\rho N\alpha_n} (\rho\xi\omega^2)\sin\alpha_n(t-\tau)d\xi d\tau \tag{20}$$

From some data available for the 105 mm system a typical angular velocity ω vs t relationship can be represented by a straight line, namely,

$$\omega(\tau) = \frac{\omega_0}{t_0} \tau \tag{21}$$

where ω_0 is the angular velocity of the shell at the exit time t_0.

Using the expression of $\omega(\tau)$ in Equation (21) and performing the integration with respect to the τ-variable, the time part of the integral in Equation (20) is obtained.

$$T(\alpha_n t) = \frac{\omega_0^2}{\alpha_n^3 t_0^2} [\alpha_n^2 t^2 - 2(1+\cos\alpha_n t)] \tag{22}$$

The integration with respect to the variable ξ is less straightforward and is therefore worked out and presented with a few details in the Appendix. Substituting Equations (22), (A4), and (A6) into Euqation (20) yields

$$\bar{u}(r,t) = \sum_{n=1}^{\infty} C_n \psi(\beta_n r) T^*(\alpha_n t) \tag{23}$$

where

$$C_n = \frac{2\omega_0^2}{\beta_n \alpha_n^6 t_0^4} \Psi(k,\beta_n) \tag{24}$$

with

$$\Psi(k,\beta_n) = \frac{k^2 \psi_2(\beta_n b) - \psi_2(\beta_n a)}{k^2 \psi_0^2(\beta_n b) - \psi_0^2(\beta_n a)} \tag{25}$$

In Equation (25) K = b/a and T* is the function inside the bracket of Equation (22),

$$\psi_0(\beta_n b) = J_0(\beta_n b) - K\ Y_0^{\cdot}(\beta_n b)$$

and

$$\psi_2(\beta_n b) = J_2(\beta_n b) - K\ Y_2(\beta_n b), \quad \text{etc.}$$

The Circumferential Displacement, v(r,t)

Let $$v(r,t) = V(r)\sin\gamma t \tag{26}$$

Substituting Equation (26) into the second equation of (4), with the Coriolis term dropped, yields

$$\frac{d^2V}{dr^2} + \frac{1}{r}\frac{dV}{dR} + (\kappa^2 - \frac{1}{r^2})V = 0 \tag{27}$$

where $\kappa^2 = \frac{\rho\gamma^2}{\mu}$.

The boundary condition at the interface between the rotating band and the shell body requires that the circumferential displacement v there vanishes to correspond to the condition of positive anchorage of the band to the shell. At the outer radius r = b it is assumed that the shearing stress is zero to correspond to a smooth contact without friction. However, since the frictional stress is dependent on the radial pressure at the interface, to introduce friction means to introduce a coupling between the radial and circumferential displacements through the boundary condition. This would make the mathematical problem unnecessarily complicated for the purpose of this analysis. A compromise approach would be to use a predetermined value of friction and thus introduce an inhomogeneous boundary condition. In this paper the zero stress condition will be used for mathematical expediency with the anticipation that the resulting shear stress may thus be lower than the actual value.

Therefore, the boundary conditions for V are:

$$V(a) = 0$$

and (28)

$$\left(\frac{dV}{dr} - \frac{V}{r}\right)_{r=b} = 0.$$

The solution of Equation (27) is

$$V(r) = B_1 J_1(\kappa r) + B_2 Y_1(\kappa r). \tag{29}$$

From the first boundary condition in Equation (28) it follows that

$$B_1 J_1(\kappa a) + B_2 Y_1(\kappa a) = 0$$

or

$$B_2 = -\frac{J_1(\kappa a)}{Y_1(\kappa a)} B_1 . \tag{30}$$

The second boundary condition leads to the following

$$B_1[b\kappa J_1'(\kappa b) - J_1(\kappa b)] + B_2[b\kappa Y_0'(\kappa b) - Y_0(\kappa b)] = 0 \tag{31}$$

Thus, the eigenvalue equation, after simplification, becomes

$$J_1'(\kappa b) Y_1(\kappa b) - Y_1'(\kappa b) J_1(\kappa b) = 0 . \tag{32}$$

Equation (32) can be further reduced by using the identities of the derivatives of the Bessel's functions.

Let $$M_n = \frac{J_1(\bar{\kappa}_n)}{Y_1(\bar{\kappa}_n)} , \quad \bar{\kappa}_n = \kappa_a$$

then Equation (32) becomes

$$J_0(k\bar{\kappa}_n) - M_n Y_0(k\bar{\kappa}_n) = \frac{1}{k\bar{\kappa}_n} [J_1(k\bar{\kappa}_n) - M_n Y_1(k\bar{\kappa}_n)] \tag{33}$$

This equation will be solved numerically to determine the values of $\bar{\kappa}_n$.

The eigenfunctions are given by

$$\psi(\bar{\kappa}_n \frac{r}{a}) = J_1(\bar{\kappa}_n \frac{r}{a}) - M_n Y_1(\bar{\kappa}_n \frac{r}{a})$$

Using $\phi(r,t) = \rho r\dot{\omega}$ in evaluating the particular integral $\bar{v}$, we have

$$\bar{v}(r,t) = -\int_0^t \int_a^{\bar{b}} \sum_{n=1}^{\infty} \frac{\xi\ \psi(\bar{\kappa}_n \frac{r}{a})\psi(\bar{\kappa}_n \frac{\xi}{a})}{\rho\ N\ \gamma_n}(\rho\ \dot{\omega})\sin\ \gamma_n(t-\tau)d\xi d\tau \tag{34}$$

The integration of the time part gives

$$T(\gamma_n t) = \frac{\omega_0}{\gamma_n t_0}\ (1-\cos\gamma_n t) \tag{35}$$

The integration with respect to ξ yields, after some elementary computation, the following expression for v.

$$v(r,t) = \sum_{n=1}^{\infty} D_n\ \psi(\kappa_n r)T^*(\kappa_n t) \tag{36}$$

where

$$D_n = \frac{2\omega_0}{\beta_n \gamma_n^2 t_0}\ \Psi(k,\kappa_n) \tag{37}$$

with

$$\Psi(k,\kappa_n) = \frac{k^2\psi_2(\kappa_n b) - \psi_2(\kappa_n a)}{(k^2 - \frac{1}{(\kappa_n a)^2})\psi_1{}^2(\kappa_n b) - \psi_0{}^2(\kappa_n a)} \tag{38}$$

In Equation (38) k = b/a and T* is the function inside the parentheses of Equation (35),

$$\psi_0(\kappa_n a) = J_0(\kappa_n a) - M_n Y_0(\kappa_n a),$$

$$\psi_1(\kappa_n b) = J_1(\kappa_n b) - M_n Y_1(\kappa_n b),$$

$$\psi_2(\kappa_n a) = J_2(\kappa_n a) - M_n Y_2(\kappa_n a),\quad \text{etc.}$$

The Axial Displacement, $w(r,t)$

Let $\quad w(r,t) = W(r) \sin pt \qquad (39)$

Substituting Equation (39) into the third equation of Equation (4) yields

$$\frac{d^2 W}{dr^2} + \frac{1}{r}\frac{dW}{dr} + (q^2) W = 0 \qquad (40)$$

where

$$q^2 = \frac{\rho p^2}{\mu} .$$

The considerations for the boundary conditions are identical with those for the circumferential displacement v. Therefore,

$$W(a) = 0 \qquad (41)$$

and

$$\frac{dw}{dr}(b) = 0.$$

The solution of Equation (40) is

$$W(r) = E_1 J_0(qr) + E_2 Y_0(qr). \qquad (42)$$

From the first boundary condition in Equation (41) it follows that

$$E_1 J_0(qa) + E_2 Y_0(qa) = 0$$

or

$$E_2 = - \frac{J_0(qa)}{Y_0(qa)} E_1 . \qquad (43)$$

The second boundary condition leads to the following.

$$E_1 J_0{}'(qb) + E_2 Y_0{}'(qb) = 0 \qquad (44)$$

The eigenvalue equation in this case is

$$J_0'(qb)Y_0(qa)-J_0(qa)Y_0'(qb) = 0 \tag{45}$$

and the eigenfunctions are

$$\psi(\bar{q}_n \frac{r}{a}) = J_0(\bar{q}_n \frac{r}{a})-L_n Y_0(\bar{q}_n \frac{r}{a})$$

where

$$L_n = \frac{Y_0(q_n a)}{J_0(q_n a)} .$$

With $\phi = \rho(\frac{b}{tg\delta})\dot{\omega}$, we have

$$\bar{w}(r,t) = -\int_0^t \int_a^b \sum_{n=1}^{\infty} \frac{\xi\psi(\bar{q}_n \frac{r}{a})\psi(\bar{q}_n \frac{\xi}{a})}{\rho\ N\ p_n}(\rho\frac{b}{tg\delta}\dot{\omega})\sin p_n(t-\tau)d\xi d\tau \tag{46}$$

The integration of the time part gives

$$T(p_n t) = \frac{b\omega_0}{(tg\delta)t_0}(1-\cos\lambda_n t) \tag{47}$$

The integration with respect to ξ yields, after some calculation, the following expression for $\bar{w}$.

$$\bar{w}(r,t) = \sum_{n=1}^{\infty} F_n\psi(q_n r)T^*(p_n t) \tag{48}$$

where

$$F_n = \frac{2\ b\ \omega_0}{(tg\ \delta)\quad p_n{}^2 t_0}\ \Psi(k,q_n) \tag{49}$$

with

$$\Psi(k,q_n) = \frac{k^2\psi_1(q_nb)-\psi_1(q_na)}{k^2\psi_0{}^2(q_nb)-\psi_1{}^2(q_na)} \tag{50}$$

where $\psi_0(q_nb) = J_0(q_nb)-L_nY_0(q_nb)$,

$$\psi_1(q_na) = J_1(q_na)-L_nY_0(q_na), \quad \text{etc.}$$

Stress Components

The rotating band is assumed to undergo elastic deformation; therefore, the stress-strain relation is given by

$$\tau_{k\ell} = \lambda e\delta_{k\ell}+2\mu e_{k\ell} \tag{51}$$

According to the pattern of deformation assumed in this analysis the components of strain are

$$e_{rr} = \frac{\partial\bar{u}}{\partial r}, \qquad e_{r\theta} = \frac{1}{2}\left(\frac{\partial\bar{v}}{\partial r} - \frac{\bar{v}}{r}\right),$$

$$e_{\theta\theta} = \frac{\bar{u}}{r}, \qquad e_{rz} = \frac{1}{2}\frac{\partial\bar{w}}{\partial r},$$

$$e_{zz} = 0, \qquad e_{\theta z} = 0$$

The corresponding stress components are:

$$\tau_{rr} = (\lambda+2\mu)\frac{\partial\bar{u}}{\partial r} + \lambda\frac{\bar{u}}{r}, \quad \tau_{r\theta} = \mu\left(\frac{\partial\bar{u}}{\partial r} - \frac{\bar{v}}{r}\right),$$

$$\tau_{\theta\theta} = (\lambda+2\mu)\frac{\bar{u}}{r} + \lambda\frac{\partial\bar{u}}{\partial r}, \quad \tau_{rz} = \mu\frac{\partial\bar{w}}{\partial r},$$

$$\tau_{zz} = \lambda\left(\frac{\partial\bar{u}}{\partial r} + \frac{\bar{u}}{r}\right), \quad \tau_{z\theta} = 0.$$

To calculate numerically the stress components, the analytical expressions must be first obtained from Equations (23), (36), and (46). The calculations involve taking derivatives of Bessel's functions of different orders. Thus, the expressions for the stresses are Bessel's functions of various combinations. They will not be given here but will be entered directly into the Fortran program written for the determination of these stresses.

COMPUTATIONAL RESULTS AND CONCLUSIONS

Three separate Fortran programs are written. One computes the radial displacement $\bar{u}$ from which the normal stresses τ_{rr}, $\tau_{\theta\theta}$, and τ_{zz} are computed, the second program computes the circumferential displacement $\bar{v}$ from which the shearing stress $\tau_{r\theta}$ is computed, and the third program computes the axial displacement $\bar{w}$ and the shearing stress τ_{rz}. A sample calculation is performed for a band a = 2.034 inch and b = 2.112 inch, with material constants E = 10^6 psi, u = .26, ρ = .000129. This sample computation is based on an angular velocity history with ω_0 = 60950 radians per second and t_0 = 0.01 second. A second calculation is made for a rotating band of the same inner radius but larger outer radius to assess the effect of the increasing thickness of the band. Results were plotted to show the variations of the stresses with the radius and also the variation of stresses with time. Figure 2 shows the three normal stresses plotted vs the radial distance between the inner and the outer radii. It is evident from the plot that the most severe normal stress component is by far the radial component σ_{rr}. All these stresses vary from tension at the inner surface of the rotating band to compression at the outer surface crossing the zero value at the midpoint of the thickness. At the outer surface the sample calculation gives a compressive stress slightly over 16,000 psi, based on a material with E = 10^6 psi and a geometry corresponding to 105 mm gun. A second sample calculation is based on the same inner radius but an increased outside radius b = 2.2374 inch. In this case the increase of radial pressure is very considerable. At the outer surface the compressive stress is increased to about 90,000 psi.

Figure 3 is a plot to give some idea about the increase of the radial stresses at the inner and the outer surfaces of the rotating band during the time period in which the angular velocity of the projectile is increased from zero to its maximum value. It can be seen that the increase of the stress is less rapid than the linear variation assumed for the angular velocity vs time function. This sample variation is quite typical for all other stress components.

Figure 4 shows the variation of shearing stresses $\sigma_{r\theta}$ and σ_{rz} vs the radial distance along the thickness of the rotating band. These stresses are two orders of magnitude smaller than the normal stresses and are considered to be slightly lower than what they should be because of the boundary conditions used in this analysis, viz., stress-free conditions. On the other hand, the normal stress components calculated are considered to be on the high side because of the zero deformation conditions assumed at the inner and outer surfaces.

To refine these results it is recommended that non-homogeneous boundary conditions be assumed in all cases. These computations can be carried out with much less effort than is involved in this analysis because the eigenvalues necessary for the computation have been calculated in the current analysis.

In conclusion, the stress distributions and their time variations in the post-engraving period of the projectile have been determined analytically. Sample calculations have been made to give numerical values of the various components of stresses. For the specific geometry and material in a particular system of gun and projectile, the Fortran programs used for the sample calculations can be used by changing the data cards to suit.

REFERENCES

1. Love, A. E. H., A Treatise on the Mathematical Theory of Elasticity, Dover Publications, New York, 1944.
2. Carslaw and Jaeger, Conduction of Heat in Solids, Second Edition, p 197, Oxford University Press, New Jersey, 1960.
3. Hilderbrand, F. B., Advanced Calculus for Applications, Prentice-Hall, New Jersey, p 177, 1962.

APPENDIX A

To evaluate the normalization constant N defined in Equation (15)

$$N = \int_a^b r\psi^2(\overline{\beta}_n \frac{r}{a})dr \tag{A1}$$

it is recalled that ψ is defined by Equation (11); thus ψ satisfies Equation (6), i.e.,

$$\frac{d^2\psi}{dr^2} + \frac{1}{r}\frac{d\psi}{dr} + (\beta^2 - \frac{1}{r^2})\psi = 0 ,$$

which can be recast in the form

$$\frac{1}{r}\frac{d}{dr}(r\frac{d\psi}{dr}) + (\beta^2 - \frac{1}{r^2})\psi = 0. \tag{A2}$$

Equation (A2) can be further changed into the form (Ref 2)

$$2r\frac{d\psi}{dr}\frac{d}{dr}(r\frac{d\psi}{dr}) + 2(\beta^2 - \frac{1}{r^2})r^2\psi\frac{d\psi}{dr} = 0.$$

Therefore,

$$\frac{d}{dr}(r\frac{d\psi}{dr})^2 + \beta^2 r^2 \frac{d(\psi^2)}{dr} - \frac{d(\psi^2)}{dr} = 0$$

and

$$\beta^2 \int_a^b r^2 \frac{d(\psi^2)}{dr}dr + [(r\frac{d\psi}{dr})^2 - \psi^2]_a^b = 0.$$

Integrating by parts, we have

$$2\beta^2 \int_a^b r\psi^2 dr = \left[r^2\left(\frac{d\psi}{dr}\right)^2 - (\beta^2 r^2 - 1)\psi\right]_a^b . \qquad \text{(A3)}$$

For β-values which are solutions of the eigenvalue equation $\psi(a) = \psi(b) = 0$, Equation (A3) is reduced to

$$\int_a^b r\psi^2 dr = \frac{1}{2\beta_n^2}\left[b^2\left(\frac{d\psi}{dr}\right)^2_{\beta_n^a} - a^2\left(\frac{d\psi}{dr}\right)^2_{\beta_n^b}\right]$$

$$= \frac{1}{2\beta_n^2}[b^2\psi'^2(\beta_n b) - a^2\psi'^2(\beta_n a)], \qquad \text{(A4)}$$

where

$$\frac{d\psi(\beta_n r)}{dr} = J_1'(\beta_n r) - KY_1'(\beta_n r).$$

Since

$$J_1'(\beta_n r) = \beta_n J_0(\beta_n r) - \frac{1}{\gamma}J_1(\beta_n r), \quad \text{etc.},$$

$$\psi'(\beta_n r) = \beta_n[J_0(\beta_n r) - KY_0(\beta_n r)] - \frac{1}{r}[J_1(\beta_n r) - \frac{1}{K}Y_1(\beta_n r)]. \qquad \text{(A5)}$$

APPENDIX B

From the formulas available in Reference (3) it is found that

$$\int_a^b \cdot \xi^2 \psi(\beta_n \xi) d\xi = \frac{1}{\beta_n}[\xi^2 \psi_2(\beta_n \xi)]_a^b \qquad \text{(B1)}$$

where $\psi_2(\beta_n\xi) = J_2(\beta_n\xi) - K\, Y_2(\beta_n\xi)$ and K is the same constant as appeared in Equation (11).

APPENDIX C

Eigenvalues

The eigenvalues for the radial displacement problem are computed from Equation (10) with the Fortran program Root and are given in the following table.

k	n = 1	2	3	4	5
1.03834	81.92742	163.85156	245.77344	327.67969	490.00000
1.10000	31.42676	62.83725	94.25140	125.66644	157.08179
1.25000	12.59004	25.14465	37.70706	50.27145	62.83662
1.66667	4.78508	9.44837	14.15300	18.86148	25.57148

The eigenvalue equation for the circumferential displacement problem as given by Equation (3) can be reduced to the following:

$$J_0(k\bar{\kappa}) - \frac{J_1(\bar{\kappa})}{Y_1(\bar{\kappa})} Y_0(k\bar{\kappa}) = \frac{1}{k}[J_1(k\kappa) - \frac{J_1(\bar{\kappa})}{Y_1(\bar{\kappa})} Y_1(k\bar{\kappa})] \qquad \text{(C1)}$$

The eigenvalue equation for the axial displacement problem after some algebraic simplification was done on Equation (45) reduces to

$$J_1(k\bar{q})Y_0(\bar{q})-J_0(\bar{q})Y_1(k\bar{q}) = 0 \qquad \text{(C2)}$$

It turns out that both Equation (C1) and (C2) give the same set of eigenvalues which will be listed below.

k	n = 1	2	3	4	5
1.03834	40.5	123.0	205.5	287.0	369.5

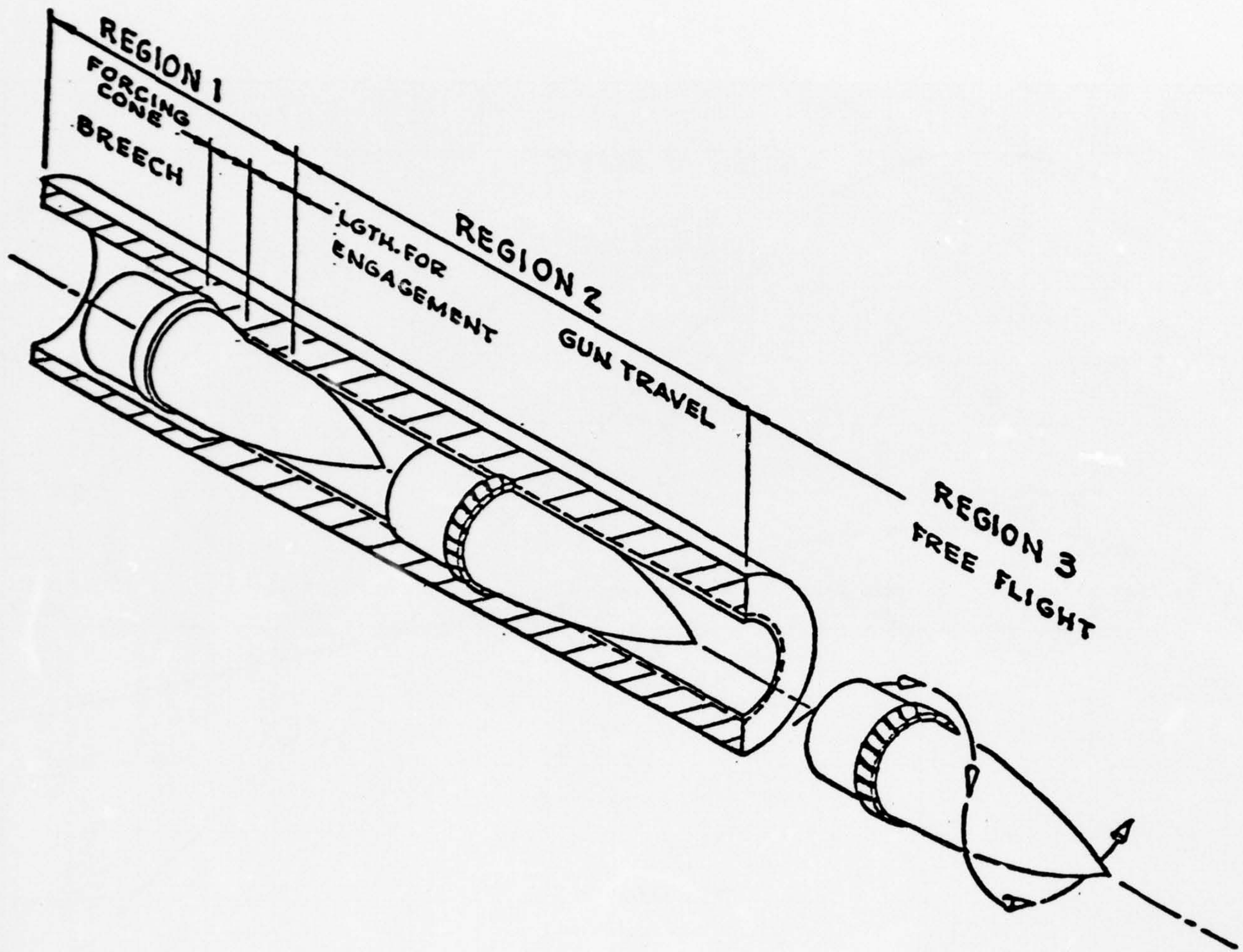

Fig 1   Various band regions in the interior ballistic cycle

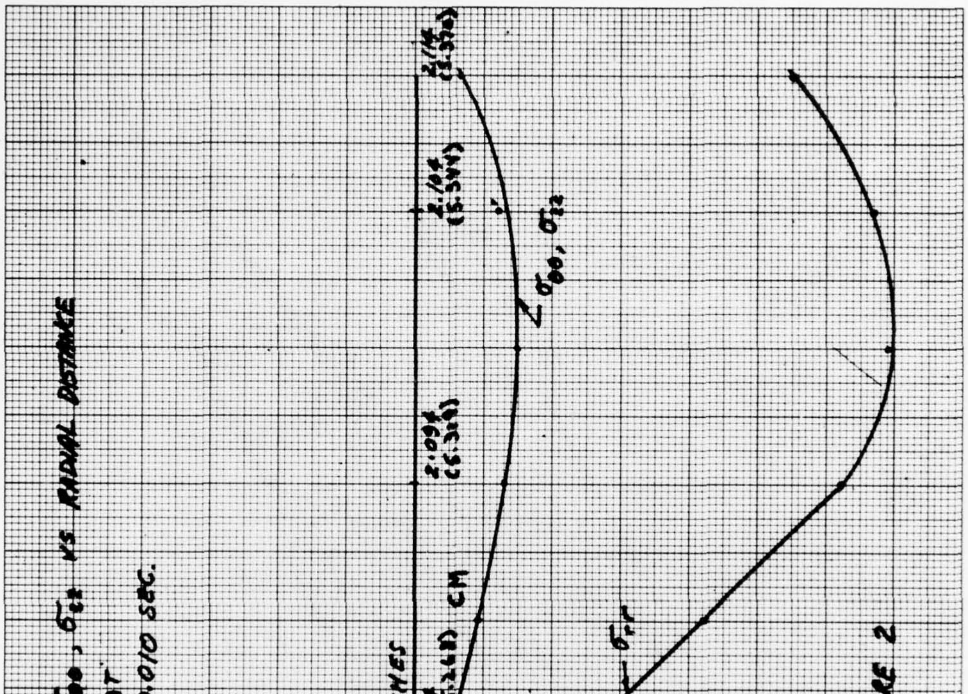
σ_{rr}, $\sigma_{\theta\theta}$, σ_{zz} VS RADIAL DISTANCE
AT
$t = 0.010$ SEC.
INCHES
CM
MPA
PSI
σ_{rr}
$\sigma_{\theta\theta}$, σ_{zz}

FIGURE 2

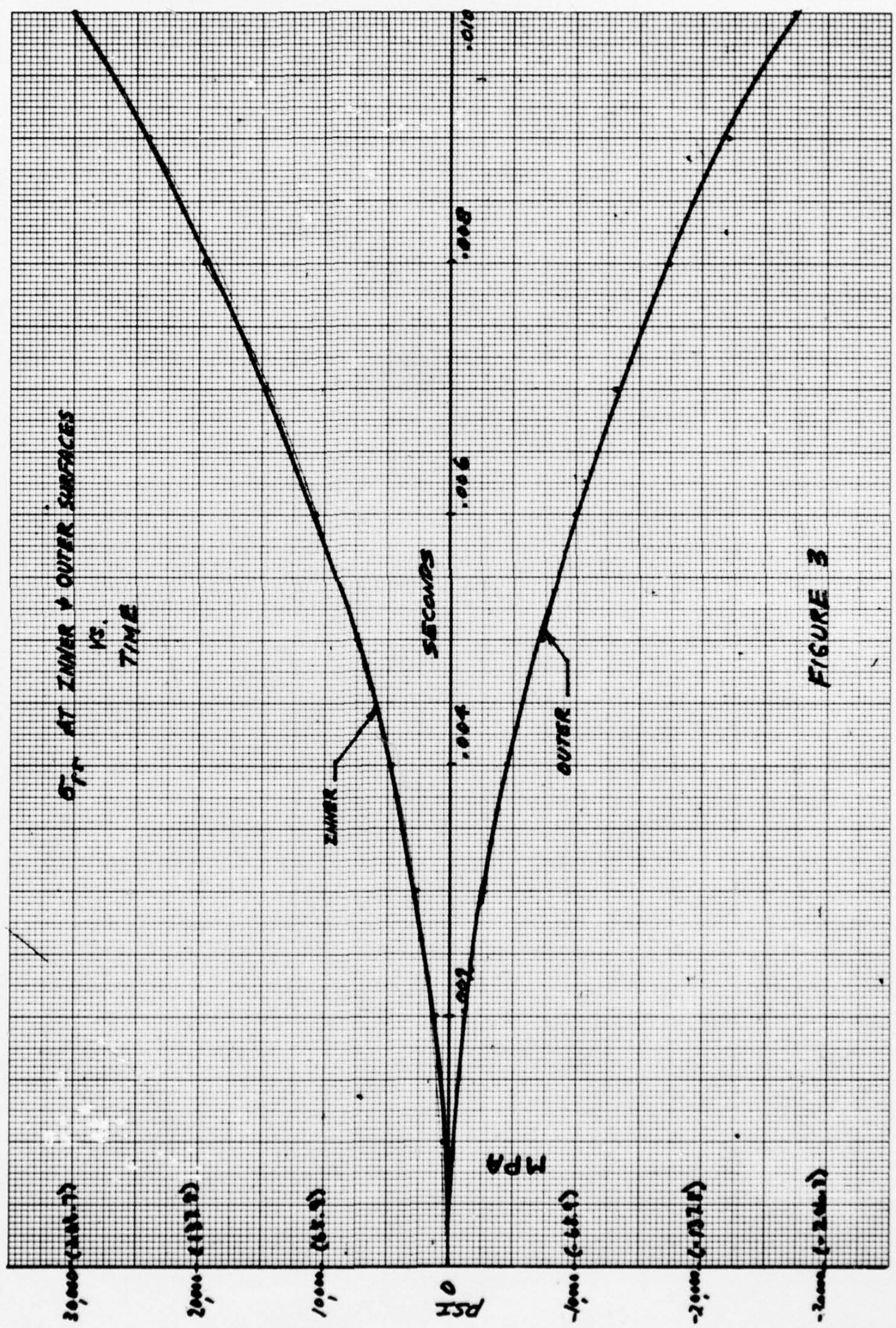
σ_{rr} AT INNER & OUTER SURFACES
VS.
TIME
SECONDS
INNER
OUTER
PSI
MPA
.002
.004
.006
.008
.010

FIGURE 3

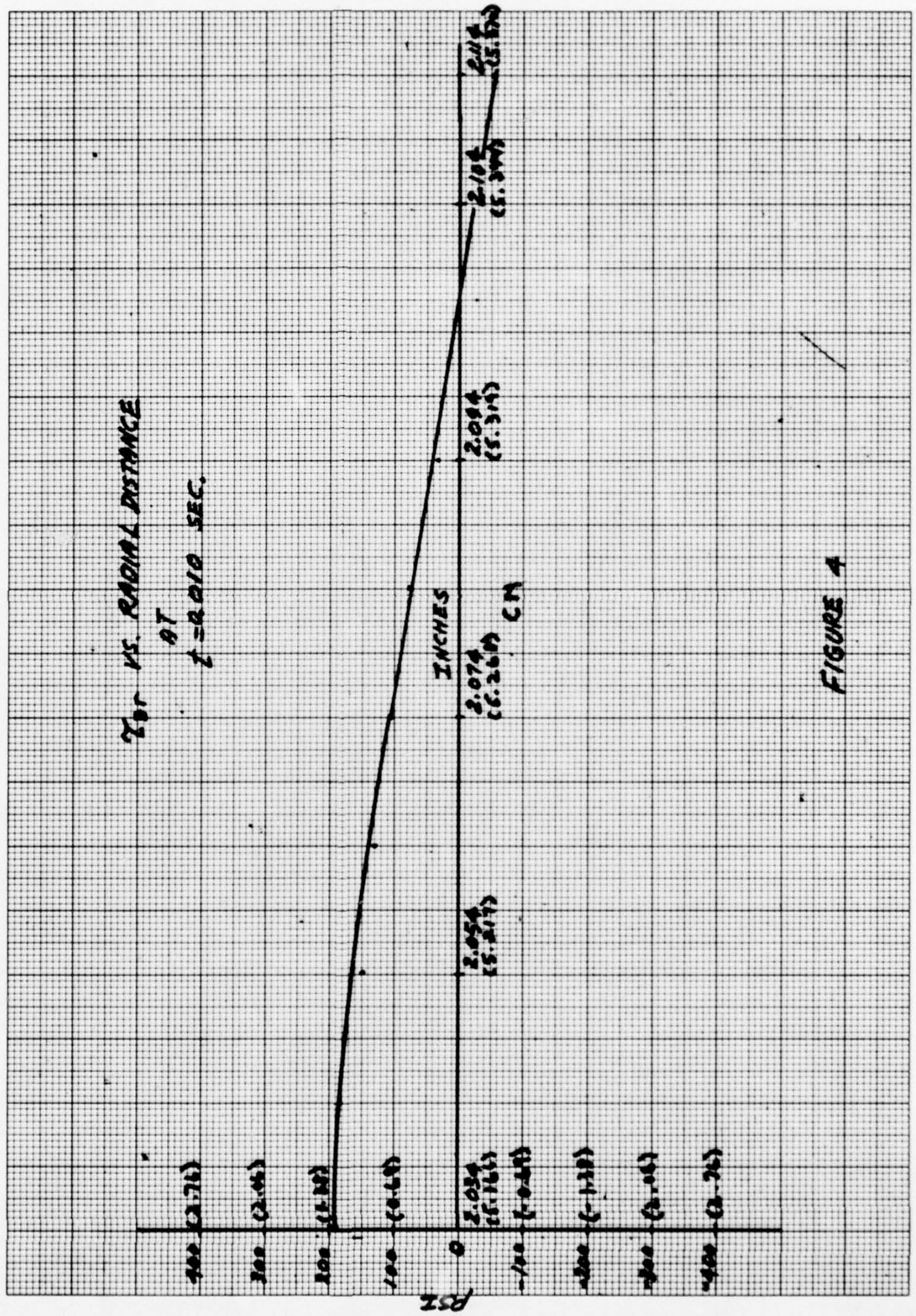
VS. RADIAL DISTANCE
AT
t = 0.010 SEC.
INCHES
CM
2.074
2.094
(5.319)
PSI
FIGURE 4

NORMAL STRESSES

```
      DIMENSION BETA(15),T(20),RA(40),SUMA(15),SUMB(15),SUMC(
     1TAUR(10,40),TAUT(10,40),TAUZ(10,40)
      READ(5,20)(BETA(I),I=2,6)
   20 FORMAT(5F10.5)
      A=2.024
      RHO=.000129
      SUMA(1)=0
      SUMB(1)=0
      SUMC(1)=0
      CC1=2017190.0
      CC2=430000.0
      CC3=1587300.0
      RPS=60955.0
      TZ=.01
      C=2.*(RPS/TZ)**2
      CM=1.03834
      SCM=CM*CM
      T(1)=0
      RA(1)=A
      DO 50 I=2,11
      T(I)=T(I-1)+.001
      DO 50 J=2,11
      RA(J)=RA(J-1)+.01
      DO 30 K=2,6
      AR1=BETA(K)
      AR2=CM*AR1
      D=.0001
      CALL BESJ(AR1,0,BJ01,D,IER)
      CALL BESJ(AR2,0,BJ02,D,IER)
      CALL BESJ(AR1,1,BJ11,D,IER)
      CALL BESJ(AR1,2,BJ21,D,IER)
      CALL BESJ(AR2,2,BJ22,D,IER)
      CALL BESY(AR1,0,BY01,D,IER)
      CALL BESY(AR2,0,BY02,D,IER)
      CALL BESY(AR1,1,BY11,D,IER)
      CALL BESY(AR1,2,BY21,D,IER)
      CALL BESY(AR2,2,BY22,D,IER)
      CT=BJ11/BY11
      X2=BJ21-CT*BY21
      X2K=BJ22-CT*BY22
      X1P1=BJ01-CT*BY01
      X1P1S=X1P1**2
      X1P1K=BJ02-CT*BY02
      X1P1KS=X1P1K**2
      CU=SCM*X2K-X2
      AR1A=AR1/A
      ALN=(CC1/RHO)**.5*AR1A
      DD=ALN**4*(SCM*X1P1KS-X1P1S)
      CN=C*CU/(DD*AR1A)
      AA=ALN*T(I)
      BB=AA**2.
      DD=COS(AA)
      TF=BB-2*(1.+DD)
      AR3=AR1*RA(J)/A
      CALL BESJ(AR3,0,BJ03,D,IER)
      CALL BESJ(AR3,1,BJ13,D,IER)
```

```
      CALL BESY(AR3,0,BY03,D,IER)
      CALL BESY(AR3,1,BY13,D,IER)
      UR=(BJ13-CT*BY13)/RA(J)
      DUR=(BJ03-CT*BY03)*AR1A
      FA=C01*DUR+C02*UR
      FB=C01*UR+C02*DUR
      FC=C02*(DUR+UR)
      CNTF=CN*TF
      SUMA(K)=SUMA(K-1)+CNTF*FA
      SUMB(K)=SUMB(K-1)+CNTF*FB
      SUMC(K)=SUMC(K-1)+CNTF*FC
   30 CONTINUE
      TAUR(I,J)=SUMA(6)
      TAUT(I,J)=SUMB(6)
      TAUZ(I,J)=SUMC(6)
      WRITE(6,40)I,J,TAUR(I,J),TAUT(I,J),TAUZ(I,J)
   40 FORMAT(1H,2X,I3,I3,5X,E15.5,5X,E15.5,5X,E15.5)
   50 CONTINUE
      CALL EXIT
      END
```

CIRCUMFERENTIAL STRESS

```
      DIMENSION BETA(15),T(20),RA(55),SUMA(15),TAUZT(10,40)
      READ(5,20)(BETA(I),I=2,8)
   20 FORMAT(7F6.1)
      A=2.024
      RHO=.000129
      CC3=793650
      RPS=60955.0
      TZ=.01
      C=2.*RPS/TZ
      CM=1.03834
      SCM=CM*CM
      T(1)=0
      RA(1)=A
      SUMA(1)=0
      DO 50 I=2,11
      T(I)=T(I-1)+.001
      DO 50 J=2,11
      RA(J)=RA(J-1)+.01
      DO 30 K=2,8
      AR1=BETA(K)
      AR2=CM*AR1
      D=.0001
      CALL BESJ(AR1,0,BJ01,D,IER)
      CALL BESJ(AR1,1,BJ11,D,IER)
      CALL BESJ(AR2,1,BJ12,D,IER)
      CALL BESJ(AR1,2,BJ21,D,IER)
      CALL BESJ(AR2,2,BJ22,D,IER)
      CALL BESY(AR1,0,BY01,D,IER)
      CALL BESY(AR1,1,BY11,D,IER)
      CALL BESY(AR2,1,BY12,D,IER)
      CALL BESY(AR1,2,BY21,D,IER)
      CALL BESY(AR2,2,BY22,D,IER)
      X2=BJ21*BY11-BJ11*BY21
      X2K=BJ22*BY11-BJ11*BY22
      CU=SCM*X2K-X2
      X1P1=BJ01*BY11-BJ11*BY01
      X1P1S=X1P1**2
      X1P1K=BJ12*BY11-BJ11*BY12
      X1P1KS=X1P1K**2
      AR1S=AR1*AR1
      CD=(SCM-1/AR1S)*X1P1KS-X1P1S
      AR1A=AR1/A
      ALN=78437*AR1A
      CN=C*CU/(QD*ALN*AR1S)
      TF=1-COS(ALN*T(I))
      AR3=AR1*RA(J)/A
      CALL BESJ(AR3,0,BJ03,D,IER)
      CALL BESJ(AR3,1,BJ13,D,IER)
      CALL BESY(AR3,0,BY03,D,IER)
      CALL BESY(AR3,1,BY13,D,IER)
      VR=(BJ13-CT*BY13)/RA(J)
      DVR1=AR1*(BJ03-CT*BY03)
      DVR2=-(BJ13-CT*BY13)/RA(J)
      DVR=DVR1+DVR2
      FA=CO3*(DVR-VR
      CNTF=CN*TF
```

```
      SUMA(K)=SUMA(K-1)+CNTF*FA
   30 CONTINUE
      TAUZT(I,J)=SUMA(6)
      WRITE(6,40)I,J,TAUZT(I,J)
   40 FORMAT(1X,I3,I3,5X,E15.5)
   50 CONTINUE
      CALL EXIT
      END
```

AXIAL STRESS

```
      DIMENSION BETA(15),T(20),RA(55),SUMA(15),TAUZ(10,40)
      READ(5,20)(BETA(I),I=2,8)
   20 FORMAT(7F6.1)
      A=2.024
      RHC=.000129
      CO3=793650
      RPS=60955.0
      TZ=.01
      C=2.*RPS/.13165*TZ
      CM=1.03834
      SCM=CM*CM
      T(1)=0
      RA(1)=A
      SUMA(1)=0
      DO 50 I=2,11
      T(I)=T(I-1)+.001
      DO 50 J=2,11
      RA(J)=RA(J-1)+.01
      DO 30 K=2,8
      AR1=BETA(K)
      AR2=CM*AR1
      D=.0001
      CALL BESJ(AR1,0,BJ01,D,IER)
      CALL BESJ(AR2,0,BJ02,D,IER)
      CALL BESJ(AR1,1,BJ11,D,IER)
      CALL BESY(AR1,0,BY01,D,IER)
      CALL BESY(AR2,0,BY02,D,IER)
      CALL BESY(AR1,1,BY11,D,IER)
      CT=BJ01/BY01
      X2=BJ11-CT*BY01
      X2K=BJ01-CT*BY02
      QU=SCM*X2K-X2
      X1P1=BJ11-CT*BY01
      X1P1S=X1P1**2
      X1P1K=BJ02-CT*BY02
      X1P1KS=X1P1K**2
      AR1S=AR1*AR1
      QD=SCM*X1P1KS-X1P1S
      AR1A=AR1/A
      ALN=78437*AR1A
      CN=C*QU/(QD*ALN*AR1S)
      TF=1-COS(ALN*T(I))
      AR3=AR1*RA(J)/A
      CALL BESJ(AR3,0,BJ03,D,IER)
      CALL BESJ(AR3,1,BJ13,D,IER)
      CALL BESY(AR3,0,BY03,D,IER)
      CALL BESY(AR3,1,BY13,D,IER)
      DWR1=AR1A*(BJ13-CT*BY13)
      DWR2=-(BJ03-CT*BY03)/RA(J)
      DWR=-DWR1+DWR2
      FA=CO3*DWR
      CNTF=CN*TF
      SUMA(K)=SUMA(K-1)+CNTF*FA
   30 CONTINUE
      TAUZ(I,J)=SUMA(8)
      WRITE(6,40)I,J,TAUZ(I,J)
```

```
   40 FORMAT(1X,I3,I3,5X,E15.5)
   50 CONTINUE
      CALL EXIT
      END
```

ROOT

```
      DIMENSION X(1000),DX(100),S(1000),DF(1000),CN(1000)
      X(1)=0.
      X(2)=41.
      DF(1)=1.0
      DX(2)=.5
      AR1=X(2)
      AR2=1.03834*AR1
      D=.0001
      CALL BESJ(AR1,1,BJ11,D,IER)
      CALL BESJ(AR2,0,BJ02,D,IER)
      CALL BESJ(AR2,1,BJ12,D,IER)
      CALL BESY(AR1,1,BY11,D,IER)
      CALL BESY(AR2,0,BY02,D,IER)
      CALL BESY(AR2,1,BY12,D,IER)
      Q=BJ11/BY11
      FA=BJ02-Q*BY02
      FB=BJ12-Q*BY12
      DF(2)=FA*AR2-FB
      DO 15 J=1,1000
      CN(J)=0
   15 CONTINUE
      S(3)=0
      DO 10 I=3,1000
      IF(CN(I). EQ. 1.) GO TO 35
      IF(ABS(DF(I-2)). LT. .0001) GO TO 35
      XD=X(I-1)-X(I-2)
      IF(S(I). EQ. 1.) GO TO 45
      IF(ABS(DF(I-1)). LT. .0001) GO TO 35
      DX(I)=DX(I-1)
      GO TO 65
   45 DX(I)=DX(I-1)*.5
   65 IF(S(I). EQ. 1.) GO TO 55
      IF(XD. GT. 0.) GO TO 35
      X(I)=X(I-1)-DX(I)
      GO TO 20
   35 X(I)=X(I-1)+DX(I)
      GO TO 20
   55 IF(XD. GT. 0.) GO TO 75
      X(I)=X(I-1)+DX(I)
      GO TO 20
   75 X(I)=X(I-1)-DX(I)
      GO TO 20
   20 AR1=X(I)
      AR2=1.03834*AR1
      CALL BESJ(AR2,0,BJ02,D,IER)
      CALL BESJ(AR1,1,BJ11,D,IER)
      CALL BESJ(AR2,1,BJ12,D,IER)
      CALL BESY(AR2,0,BY02,D,IER)
      CALL BESY(AR1,1,BY11,D,IER)
      CALL BESY(AR2,1,BY12,D,IER)
      FA=BJ02*BY11-BJ11*BY02
      FB=BJ12*BY11-BJ11*BY12
      DF(I)=FA*AR2-FB
      IF(ABS(DF(I)). LT. .0001) GO TO 100
      DD=DF(I)*DF(I-1)
      IF(DD. GT. 0.) GO TO 90
```

```
      S(I+1)=1.0
      GO TO 10
   90 S(I+1)=0.
      GO TO 10
  100 WRITE(6,150)X(I)
  150 FORMAT(F10.5)
      CN(I+1)=1.
      CN(I+2)=1.
      DX(I+1)=.05
      DX(I+2)=.05
   10 CONTINUE
      CALL EXIT
      END
```

DISTRIBUTION LIST

	Copy No.
Commander	
U.S. Army Armament Research and Development Command	
ATTN: DRDAR-LCA, Dr. E. Sharkoff	1
DRDAR-LCF-A, Mr. G. Demitrack	2
DRDAR-LCA-OK, Mr. H. Pebly	3
DRDAR-LCA-OP, Mr. M. Eig	4-7
DRDAR-TSS	8-12
Dover, NJ 07801	
Director	
U.S. Army Materials and Mechanics Research Center	
ATTN: DRXMR, Dr. E. Wright	13
DRXMR-R, Dr. G. Thomas	14
DRXMR-TE, Dr. E. Lenoe	15
Watertown, MA 02171	
Defense Documentation Center	16-27
Cameron Station	
Alexandria, VA 22314	